Ocean Engineering 97 (2015) 175–185

Contents lists available at ScienceDirect

Ocean Engineering

journal homepage: www.elsevier.com/locate/oceaneng

Spatial variability of extreme wave height along the Atlantic and channel French coast

Alexandre Nicolae Lerma*, Thomas Bulteau, Sophie Lecacheux, Déborah Idier

BRGM (French Geological Survey), Risks and Prevention Division—Coastal Risks and Climate Change Unit, 3 avenue Claude Guillemin, BP36009, 45060 Orléans, France

ARTICLE INFO

Article history:
Received 27 June 2014
Accepted 31 January 2015
Available online 20 February 2015

Keywords:
Extreme statistics
Double threshold
Reproducibility
Historical events
BoBWA-10 kH
BoBWA-X

ABSTRACT

The knowledge of wave climate, and more particularly of the extremes and historical large wave events, is crucial for offshore infrastructure design as well as coastal applications such as defences design or submersion and erosion risks assessment. When it comes to analysing the spatial variability of extremes, a key issue is to ensure a uniform approach to get spatially comparable results. The present paper describes a new wave extreme values database for the French Atlantic and Channel coasts (BoBWA-X) relying on: (1) the wave hindcast BoBWA-10 kH (1958–2002; Charles et al., 2012. J. Clim. 25 (6), 2020–2039. doi:10.1175/JCLI-D-11-00086.1); (2) a POT/GPD method adapted to reduce the operator subjectivity in the threshold choice so as to ensure reproducible and comparable results along the coasts. The obtained extreme wave heights of 43 points distributed along the coast, exhibit a significant spatial variability delimiting 4 relatively homogenous areas, with 100-year return wave heights ranging between 3 m (East Cotentin) and 16 m (Western Brittany). These spatial distributions are analyzed in terms of spatial variability of the statistical parameters, using a depth-independent analysis and 7 quite homogeneous coastal segments are identified. The delimited segments are directly related to the wave climate and the exposure to classical storm waves. Therefore, they show similar repartition frontiers with the delimited areas by the H_{s100} spatial variations but with a higher degree of precision. The analysis of past events over the 1958–2002 period of the BoBWA-10 kH dataset shows 7 events characterized by wave heights with return periods larger than 50 years. The extent and intensity of these events vary greatly from one zone to another. For instance, the 1979 event affected 950 km of coast. Brittany is a particularly exposed region, with two events (1958, 1990) whose H_s return period ($R_p(H_s)$) ranges between 70 and 100 years. The highest return period is detected in the Dover Strait area ($R_p(H_s)=$ 107 years) during the Daria storm (January 25th 1990). The spatial variability of these large wave events is discussed regarding the atmospheric conditions and their similarities with classical weather types. Both databases (BoBWA-10 kH and BoBWA-X) are available at http://bobwa.brgm.fr.

1. Introduction

Accurate knowledge of extreme wave heights and their return periods is of critical importance for the design of offshore infrastructure, coastal defences or assessments of submersion and erosion risks. Large wave events are frequently associated with severe weather conditions such as storms circulating directly to the coast or occasionally far from the point of interest. When considering several sites, the definition and characterization of large wave events can vary widely, depending on the sites exposure and on average wave patterns.

Today, studies analysing significant wave height (H_s) extreme values at local scales are performed routinely, providing data on wave conditions for different return periods according to specific coastline characteristics (e.g. Méndez et al., 2006; Martucci et al., 2010). However, results are dependent on the initial data and the selected statistical methods (Mathiesen et al., 1994). Consequently, return values obtained for a same point but from different studies can vary widely (e.g. Bulteau et al., 2013a), making them difficult to interpret.

One approach to deal with this issue is the Regional Frequency Analysis (RFA). It consists in pooling together observations from several sites inside a homogeneous region, assuming that the highest observations in that region follow a common regional

* Corresponding author. Tel.: +33 2 38 64 34 11.
E-mail addresses: a.nicolaelerma@brgm.fr (A. Nicolae Lerma), t.bulteau@brgm.fr (T. Bulteau), s.lecacheux@brgm.fr (S. Lecacheux), d.idier@brgm.fr (D. Idier).

http://dx.doi.org/10.1016/j.oceaneng.2015.01.015
0029-8018/

probability distribution, up to a local scale factor representing specific characteristics of each site (Bernardara et al., 2011). This approach can reduce uncertainties and was recently set up to estimate extreme marine water levels (Duluc et al., 2014; Weiss et al., 2014b) and extreme significant wave heights (Weiss et al., 2014a). It is especially useful when dealing with short times series as it artificially increases the duration of observation. However, this approach raises the issues of the definition of homogeneous regions and the inter-site dependency.

Another approach entails treating local points of a given dataset with a homogenous statistical method, enabling one to delineate *a posteriori* homogeneous areas in terms of extremes. A prerequisite to this method is the availability of long term and homogenous databases at regional or national scale to properly consider the variability of wave characteristics along the coasts (Neelamani et al., 2007; Méndez et al., 2011; Reguero et al., 2013). Such databases are now available thanks to the production during the last decade of global or regional wave hindcasts through wind wave numerical modeling based on meteorological reanalysis.

There are many parametric statistical laws that can be used to determine extreme values from a sample of data. Generally, the most relevant statistical law and method are selected according to the specific distribution characteristics. Those mainly used are the Generalized Extreme Value (GEV) distribution which is theoretically applied to a set of maximum values per block (BM sample) and the Generalized Pareto Distribution (GPD), applied to a sample of POT values (Peaks-Over-Threshold). The method most commonly recommended for wave distribution analysis uses the POT/GPD approach (Hawkes et al., 2008; Li et al., 2012). The advantage is that all the high values for the period under study are taken into consideration to adjust the parametric distribution, which is not the case with the BM/GEV approach where only one value per year is considered (for classic processing of yearly maxima). The POT/GPD approach therefore produces more accurate estimations of extreme values, especially when the data sample does not cover many years. It is based on choosing a threshold u above which the events are selected. The results obtained are thus highly dependent on the chosen threshold, this last being strongly influenced by the operator's subjectivity (Hawkes et al., 2008; Li et al., 2012). The variability of results obtained between two studied points can therefore be due not only to the characteristics of the data, but also to the way the threshold values are chosen (Neelamani, 2009; Thompson et al., 2009). To ensure that the results from the recording points are comparable, subjectivity in the choice of the threshold must be reduced as far as possible.

The aim of this article is to build a new homogeneous extreme wave atlas allowing inter-comparisons of extreme values along the French Atlantic coastline including the Bay of Biscay and Channel coastline. The issue of threshold subjectivity is tackled with the implementation of an iterative method combining the double-threshold approach put forward by Bernardara et al. (2014) with several visual and statistical tests. The selected homogeneous wave dataset is the BoBWA-10 kH retrospective simulations database (Charles et al., 2012).

After presenting the data (Section 2) and the methodology (Section 3), the creation of the BoBWA-X database is detailed (Section 4). Section 5 provides an analysis of the spatial variability of extreme wave characteristics and past large wave events. The uncertainties associated with the method and the data are discussed in Section 6 before drawing the conclusion (Section 7).

2. Data

BoBWA-10 kH wave hindcast covers 44.7 years from January 1958 to August 2002 (Charles et al., 2012). This database was built up from the WaveWatch III model (Tolman, 2009) in a two-way nested configuration, with the parameters given by Ardhuin et al. (2009). The model was forced by ERA-40 wind reanalyses (Uppala et al., 2005) every 6 h at a height of 10 m across a 1.125° × 1.125° grid, and covers the North Atlantic (spatial resolution of 0.5°) and the French Atlantic and Channel coasts (spatial resolution of 0.1°). A calibration was carried out by varying the wind input height and comparing the simulated waves against the Biscay buoy measurements over the period 1998–2002. The optimal wind input height value was found to be 4.5 m. This calibration indirectly compensates the known underestimation of winds by ERA-40 reanalyses.

The validation performed by Charles et al. (2012) for 9 buoys (orange crosses, Fig. 1, Brittany buoy not shown) concurred well with observations ($0.76 < R^2 < 0.94$). Paris et al. (2014) showed that, in the Bay of Biscay area, BoBWA-10 kH had the lowest statistical errors compared to the other available regional wave hindcast databases (CERA-40, Caires and Sterl, 2005; ANEMOC, Benoit et al., 2006; ERA-INTERIM, Dee et al., 2011; Bertin and Dodet, 2010). Comparisons with 5 buoys data (purple circle, Fig. 1, plus Brittany buoy) show that the highest wave height values (above the 90th percentile) are reproduced more accurately (Fig. 2). For more details about BoBWA, see (Charles et al., 2012) and http://bobwa.brgm.fr.

To complete the validation for extreme statistics application, we compared BoBWA-10 kH data with observations made during large wave events. A large wave event is defined as an event for which the period in which H_s is larger than 2/3 of the maximum value reached during the entire record. Observations and model outputs are compared at two buoy locations (one offshore: Biscay; one nearshore: Minquiers, in the western part of the English Channel). We detected 9 events at the Biscay buoy (from 1998 to 2002), and 7 events at the Minquiers buoy (from 1992 to 1994 and from 1997 to 2002). Only the storm peaks (highest observed and

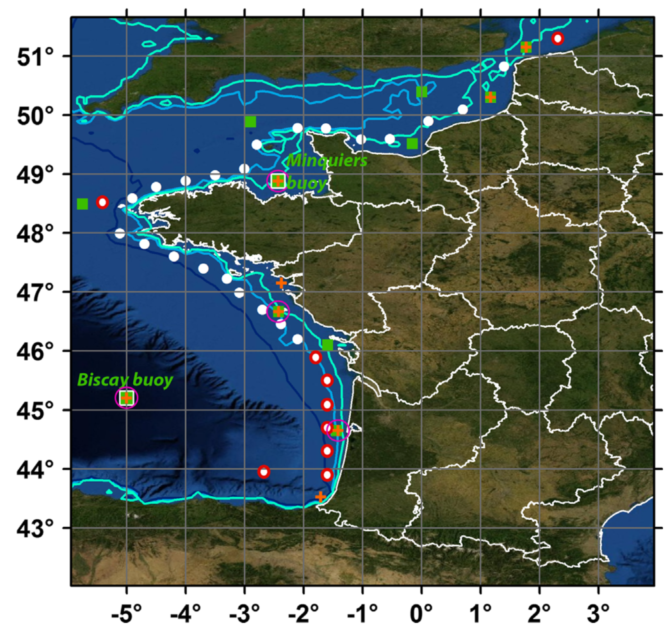

Fig. 1. Location of selected points for the statistical analysis: grid points with 6-hourly data (white circles) and data buoys (green squares). Red circles show points for dual analysis (hourly and 6-hourly data). In addition, BoBWA-10 kH validation points are identified (orange crosses) as well as points used for the comparison of BoBWA-10 kH with the other available regional wave hindcast databases (purple rounded squares). Last, squares with white edges identify the two buoys used in the present study to assess the ability of BoBWA-10 kH to reproduce the highest wave heights. The contour lines show the 30 m isobath (light blue), 50 m isobath (blue) and 100 m isobath (dark blue). (For interpretation of the references to color in this figure legend, the reader is referred to the web version of this article.)

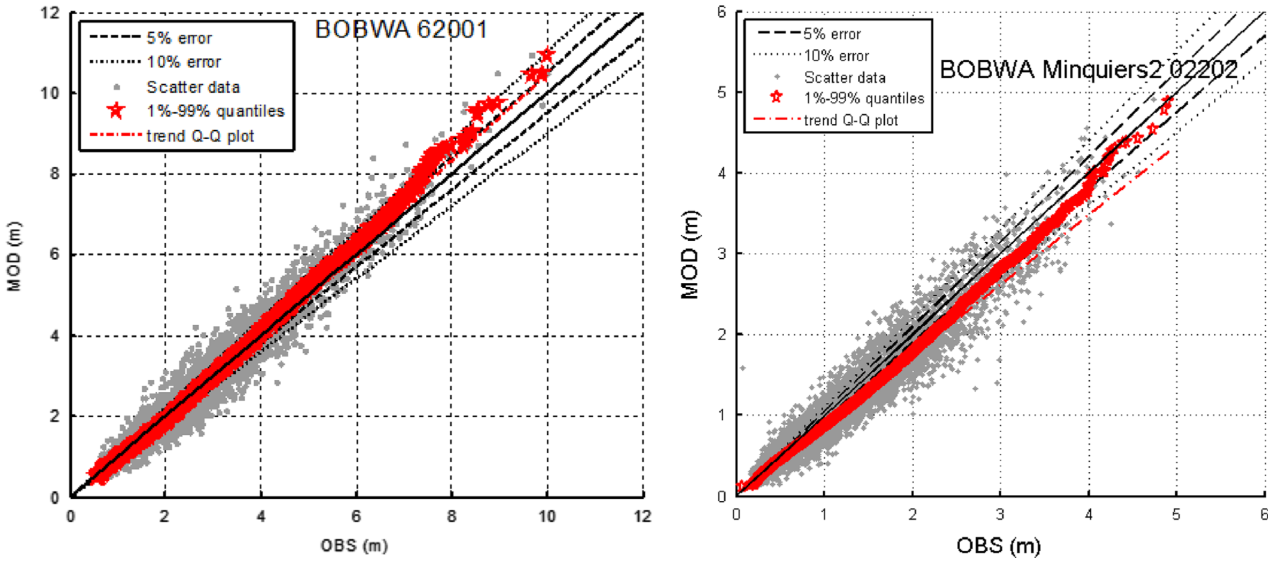

Fig. 2. BoBWA-10 kH performance for the H_s parameter, for the Biscay (left) and Minquiers (right) buoys. The dispersion diagram (gray) is superimposed over the linear trend for H_s quantiles (red), from Lecacheux and Paris (2013). (For interpretation of the references to color in this figure legend, the reader is referred to the web version of this article.)

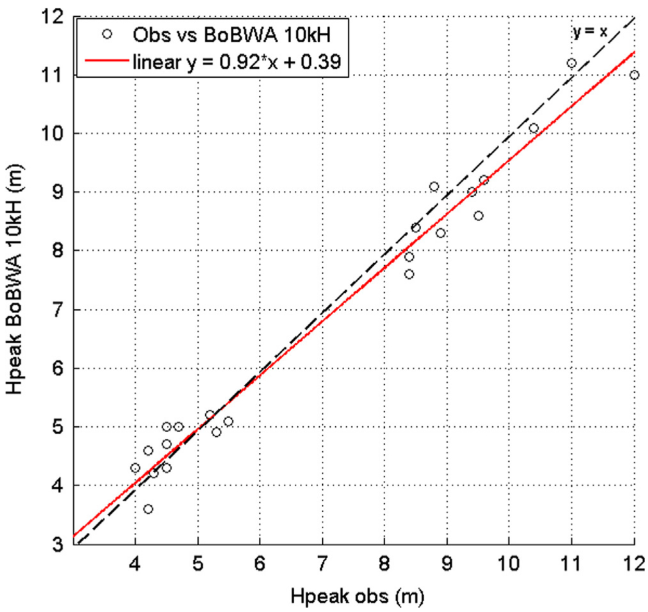

Fig. 3. Observations versus simulations for the Biscay and Minquiers buoys for selected strong swell events (H peak: local maximum value of H_s during a strong swell event), $R^2 \sim 0.98$; RMSE = 0.47 m, NRMSE = 5.9%.

simulated H_s values, without consideration of possible temporal gap ± 2 h) were considered (see Fig. 3). Because no independence criteria were used for this event analysis, 2 or 3 peaks were taken for some events, making a total of 22 peaks. It is worth recalling here that we want to characterize the ability of BoBWA-10 kH to correctly reproduce large wave heights. Therefore, the more peaks the better to make a sound assessment.

The results show a high correlation between simulations and observations of the storm peaks ($R^2 \sim 0.98$; RMSE = 0.47 m; NRMSE = 5.9%). We found a mean relative error of 4.3% (between 0.3 m and −1 m) for the Biscay buoy and a null mean relative error for the Minquiers Buoy, with differences ranging from −0.5 to 0.6 m.

Thus, the BoBWA-10 kH data fit well with observations for both the 90% quantile and peak heights during high-energy events. These findings indicate that the BoBWA-10 kH database can be used to produce sound statistics on extreme wave heights.

3. Method

3.1. Theoretical model

The approach developed in our study relies on the use of a single distribution function, the GPD, and subsequent spatial comparisons of significant wave height values (H_s) recorded at the different analyzed points.

For a given threshold u, the GPD is written as follows (Eq. (1)):

$$\left[\begin{array}{ll} P(H_s \le x | H_s > u) = 1 - \left(1 + \frac{\xi(x-u)}{\sigma}\right)_+^{-1/\xi} & \text{if } \xi \ne 0 \\ P(H_s \le x | H_s > u) = 1 - \exp\left(-\frac{(x-u)}{\sigma}\right) & \text{if } \xi = 0 \end{array}\right.$$

where $x > u$ and where $s_+ = \max(s, 0)$ with the notation $s_+ = \max(s, 0)$, $s \in \mathbb{R}$.

ξ and σ are, respectively, the shape and scale parameters under the GPD. When applying the GPD, the implicit assumption is that the number of events occurring in a fixed interval of time follows a Poisson distribution (Coles, 2001).

The main difficulty when using a GPD model lies in choosing the most relevant threshold. Two criteria have to be met to identify a suitable threshold. The value selected for the threshold u must be: (1) low enough to ensure that there are enough points to support a proper fit of the distribution, and thus limit variance; (2) high enough to be within the model's range of asymptotic validity and thus limit bias. Graphical tools such as mean residual life plot and modified scale and shape parameters plot are classically used to help selecting an appropriate threshold (Coles, 2001; Li et al., 2012). However, the subjectivity of the operator remains often involved leading to potentially non-reproducible results. To ensure that results from several different points are comparable and as reproducible as possible, we must limit the subjectivity related to the threshold choice. Bernardara et al. (2014) recommended a double-threshold (u_p, u_s) method to deal with auto-correlated environmental variables in a POT framework. We adapted this method for our study of extreme significant wave heights (see sections below) to come up with an iterative approach using a series of visual and statistical tests.

The successive steps for extreme significant wave heights analysis are:

- A directional analysis of waves to ensure homogeneity of the dataset (Section 3.2);
- Physical declustering by selecting a proper physical threshold u_p (Section 3.3);
- Statistical optimization in selecting iteratively a relevant value of the statistical threshold u_s (Section 3.4 and Fig. 4).

3.2. Directional analysis

Statistical analyses of extreme H_s values require a sample of independent and identically distributed events. To meet this second criterion, the first step in applying the method is to isolate homogeneous events within a time series of wave heights. A directional analysis is performed to determine whether the high H_s values are associated with a single directional sector or with several discontinuous directional sectors. In the second case, this would mean that large wave in two different sectors are generated by weather systems of different origins and exerting different influences. Consequently, each group of large wave must be treated separately from the others because their distributions may not be identical.

3.3. Physical declustering and choice of the u_p threshold

The second step is to select independent large wave events using the POT method. To do so, a threshold up is set, above which only the maximum H_s value is selected for each event that exceeds this threshold. The independence of the maximum H_s selected is ensured by setting a minimum interval between peak wave heights. This interval may vary depending on the characteristics

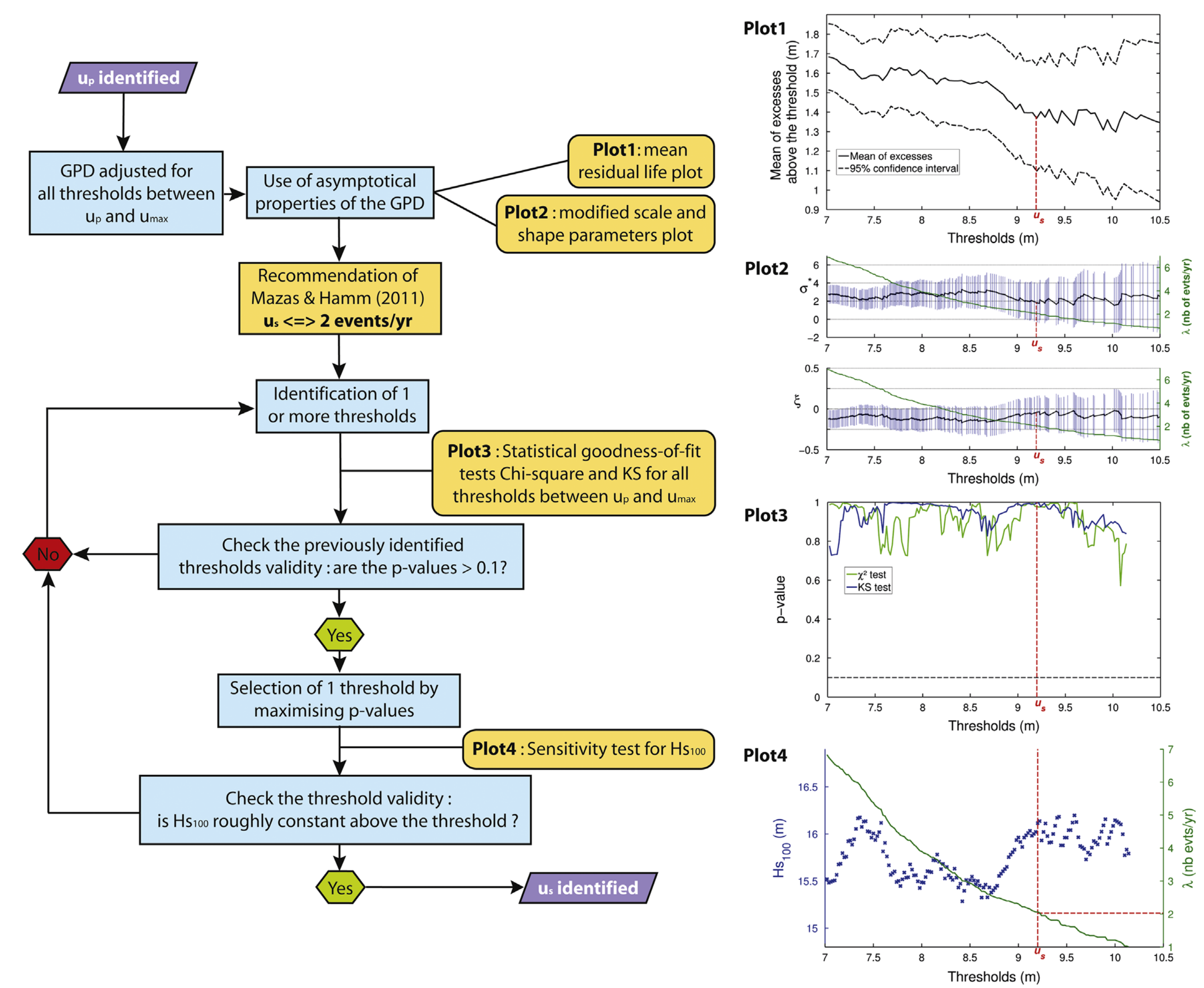

Fig. 4. Flow chart showing the iterative methodology used to identify u_s (example from the Biscay buoy point). The four graphs on the right were used successively to select the best threshold. **Plot1**: We looked for the lowest threshold for the highest domain of linearity. The dotted lines show the boundaries of the 95% confidence interval. **Plot2**: we looked for the lowest threshold for the highest domain of stability for ξ and σ^*. The vertical blue bars show the 95% confidence intervals. The green lines belong to the secondary y axis and indicate the number of events per year (λ) corresponding to each threshold. Several candidate thresholds could be chosen from Plots 1 and 2. **Plot3**: we discarded a threshold if the statistical tests (chi-square and Kolmogorov–Smirnov) failed (i.e. p-value < 0.1) and identified a single threshold by maximising the p-values. **Plot4**: final visual check before final rejection or acceptance of the threshold selected previously. Shown here are the results for the Biscay_09 point as an illustration. $u_p = 7$ m and $u_{max} = 10.2$ m (corresponding to a frequency λ of 1 event per year).

of observable weather conditions along the coastline under study (Morton et al., 1997; Li et al., 2012, 2014). The value for the up threshold is set so that a sample of several hundred peak values can be selected to include both moderate and strong storm events (Mazas and Hamm, 2011). In practice, this corresponds to a number of events per year λ_p between 5 and 10 in average. A statistical adjustment test for χ^2 (Greenwood and Nikulin, 1996) is performed to verify that the annual occurrence of peak wave heights in the resulting sample follows a Poisson distribution (with a 0.1 level of risk). If not, a higher physical threshold must be selected. The GPD can thus be adjusted, theoretically, to the data whenever the us threshold is equal to or higher than up.

3.4. Determination of the u_s threshold for the GPD

The u_s threshold (for the GPD) is selected by iteration (Fig. 4). First, the two classic visual tests based on the asymptotic properties of the GPD (Coles, 2001), and presented in Section 3.1, are performed: if the average of excesses of H_s above u varies linearly with u (i.e. mean residual life plot, plot 1 in Fig. 4) when $u > u_s$, and if the modified scale parameter $\sigma^* = \sigma - \xi u$ and the shape parameter ξ remain constant with any threshold u which is higher than u_s (i.e. plot 2 in Fig. 4), then u_s is a good candidate threshold. In practice, the GPD is adjusted to the data for all thresholds within the range between u_p and a threshold $u_{\max}$ that corresponds to $\lambda_{\min} = 1$ event per year on average (Mazas and Hamm, 2011). The curves plotted in these two graphs are rarely unambiguous and the choice of one threshold or another based on these tests alone is often subjective. The practical recommendation developed by Mazas and Hamm (2011) is then applied: for a number of years represented by a large enough sample (more than 40 years, which is the case with BoBWA-10 kH), the u_s threshold should correspond to $\lambda_s \simeq 2$ events a year on average. Based on the graphs and on this recommendation, one or more potentially valid thresholds can then be selected.

Two statistical adjustment tests (χ^2 with 10 classes and Kolmogorov–Smirnov (KS), Shorack and Wellner (2009)) are then performed for all of the thresholds between u_p and $u_{\max}$, and the p-value variations are plotted according to the threshold for each of the tests. In a statistical adjustment test, the p-value represents the probability of obtaining a value equal to or higher than the test statistic, given a null hypothesis (i.e., where the data sample effectively conforms to the distribution being tested). If the p-value is below a predetermined level of risk, the null hypothesis is rejected. The thresholds identified previously can thus be validated visually (when the p-value is higher than the level of risk set at 0.1) and a choice between several thresholds candidates can be made (searching for maximum p-values). If at least one of the two p-values for the threshold considered is lower than the 0.1 level of risk, that threshold value is rejected and a different one may have to be chosen by reviewing the full set of graphs, Plot1, Plot2 and Plot3 (Fig. 4).

To complete the analysis, a sensitivity graph is plotted to show the variations in the 100-year value of H_s (H_{s100}) according to the threshold selected (i.e. plot 4, Fig. 4). The value of this type of graph is discussed in Mazas and Hamm (2011). If the threshold has been chosen appropriately, H_{s100} should remain relatively constant for thresholds above u_s. If it does not, a higher threshold must be selected and the process repeated.

If the iterative process we have described here fails to identify one single threshold u_s after tests have been performed on all the possible thresholds, then the method is considered not applicable to the sample in question. Although we did not encounter this situation, should it arise the principle would be to establish a final threshold chosen subjectively. In addition to the graphs Plot1, 2, 3, 4, a visual comparison of Probability–Probability and Quantile–Quantile plots for each candidate threshold might be helpful.

3.5. Method for estimating GPD parameters and uncertainties

The GPD parameters (see Eq.(1)) have to be estimated according to the specific characteristics of the data analyzed. Among the numerous methods for estimating GPD parameters, the most commonly used are the MOM (moments), PWM (probability weighted moments) and ML (maximum likelihood) methods (Mackay et al., 2011). The method used will have a significant impact on the results, and must therefore be chosen with care. As a rule, it is a good idea to test several estimation methods and to choose the one that produces the best fit. However, if the aim is to make a spatial comparison of results, only one method for estimating the parameters should be used for all the study sites. As guidelines, according to comparisons by Mackay et al. (2011) between several methods for estimating GPD parameters, MOM is the most appropriate for data samples with a size n to 100 and a negative shape parameter ξ (which refers to a bounded distribution). In those cases, the estimators calculated with MOM are indeed among those with the smallest bias and root mean square errors (RMSE). The method selected for the present study is given in the application section (Section 4).

The confidence intervals for the extreme values at each point studied are calculated by the Delta method (Coles, 2001) to characterise the sampling uncertainty. This uncertainty depends on the data but also on the probability distribution used.

4. The BoBWA-eXtremes database

The method for choosing the threshold (u_s) was applied to 43 analysis points located along the French Atlantic around 100 and 50 m depth on the Bay of Biscay coasts and between 50 and 30 m depth on the Channel coasts (see Fig. 1). To make comparisons easier, the values shown are those obtained with 6-hourly time series of all directional sectors. At last, it is worth specifying that among the analyzed points, only three of them located in the East part of the English Channel had two directional sectors for larges waves.

The GPD parameters were estimated using the method of moments (MOM). Indeed, in our study, the shape parameter ξ is always negative, and if the recommendation of Mazas and Hamm (2011) is applied (i.e., u_s should correspond to $\lambda_s \simeq 2$ events per year on average, in practice, the mean over the 43 points is $\lambda_s \simeq 2.3 \pm 0.4$), the final number of points for GPD adjustment is $n = 2 \times 44.64 \approx 90$. Thus, for the present dataset, following Mackay et al. (2011), MOM is the most appropriate method to estimate the statistical parameters.

The uncertainty associated with u_s selection and the use of the method of moments to estimate GPD parameters was assessed in the light of the maximum difference obtained in relation to the 100-year value, for example, from all the GPD adjustments performed (thresholds between u_p and $u_{\max}$, Fig. 5). For all of the points analyzed, the difference is less than 10% and averages 6.7%.

The physical threshold u_p used for declustering varies according to the considered study point. As described in Section 3.3, we selected u_p so that the resulting number of events per year λ_p was between 5 and 10 in average, which is physically sounding for the region. Also, depending on the result of the statistical test used to check the conformity of the number of occurrences to a Poisson distribution, it was sometimes necessary to make u_p vary, which in return, changes λ_p. As a result, the mean of λ_p over the 43 points is $6.6 \pm \pm 1.7$.

In our study, a sensitivity test was performed to measure the possible impact of a variation in the minimum interval set between two successive peaks during the selection of independent events using the POT method (physical declustering, see Section 3.3). For the data we processed, the minimum interval between two successive peaks was set to vary from 48 to 72 h. No significant differences were observed in the end results. A 72-h period was therefore chosen, to guaranty the independence criteria in case of very long storms. Finally, for all of the points analyzed, the bounds of the relative 95% confidence interval calculated by the Delta method (Coles, 2001) for H_{s100} were comprised within $\pm 10\%$ of that value.

With the method we applied, the uncertainty arising from subjectivity in the choice of the statistical threshold was greatly reduced. When applied by different operators, the method resulted virtually systematically in the same choice of thresholds, underscoring its robustness and reproducibility and the comparability of results. Thanks to the close match between the BoBWA-10 kH data and the field observations, we were able to create a robust regional database on extreme local conditions (BoBWA-X, Bulteau et al., 2013a) based on a realistic dataset. The statistical results obtained for all of the points are summarized in data sheets available at (http://bobwa.brgm.fr). As the statistical analysis phase was performed in a homogeneous manner for all of the study sites (one distribution, one parameters' estimation method, a uniform way to select the physical threshold u_p and obtain independent and identically distributed (i.i.d) POT events, a robust iterative method to derive extreme values limiting the operator subjectivity in the choice of the statistical threshold (u_s), we claim that this protocol is designed to allow comparisons between local results and to highlight the spatial variability of extreme wave characteristics on regional scales.

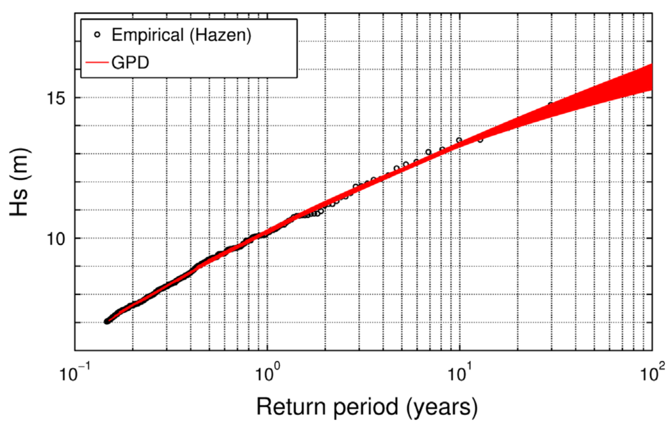

Fig. 5. GPD adjustment using the method of moments for all thresholds between u_p and $u_{max,}$ example for the Biscay buoy. The maximum relative error for H_{s100} is around 7% of the final result.

5. Spatial analysis of extreme values and past events

Among the analyzed points, only three of them, located along the English Channel, had two directional sectors for large waves. To facilitate comparisons, the values shown in this section are those obtained with 6-hourly time series of all directional sectors.

5.1. Spatial variability of statistical parameters and H_{s100}

Before observing the spatial variability it is important to recall that even if we attempted to select points with homogeneous criteria of depth (around 50 m, in order to ensure to be localized before the depth-induced wave breaking limit), because of the regular mesh grid and given that the seabed along the eastern Channel coast is at a maximum depth of around 30 m, it was not possible to comply systematically with this principle.

Thus, the spatial distribution of significant wave heights for 100-year return period is necessarily influenced by the location depth in addition to the exposure of each point to waves. Fig. 6a shows the spatial variations of the 100-year return values of significant wave heights along the Atlantic and Channel coasts (H_{s100}). Only the nearshore analyzed points are represented. Four areas with similar extreme wave characteristics can be distinguished:

- The Channel east of the Cotentin peninsula, where the values are the lowest ($H_{s100} \approx 3$–6 m);
- Western Brittany, which has the highest values obtained from the statistical analysis ($H_{s100} \approx 16$ m) and a similar eastward

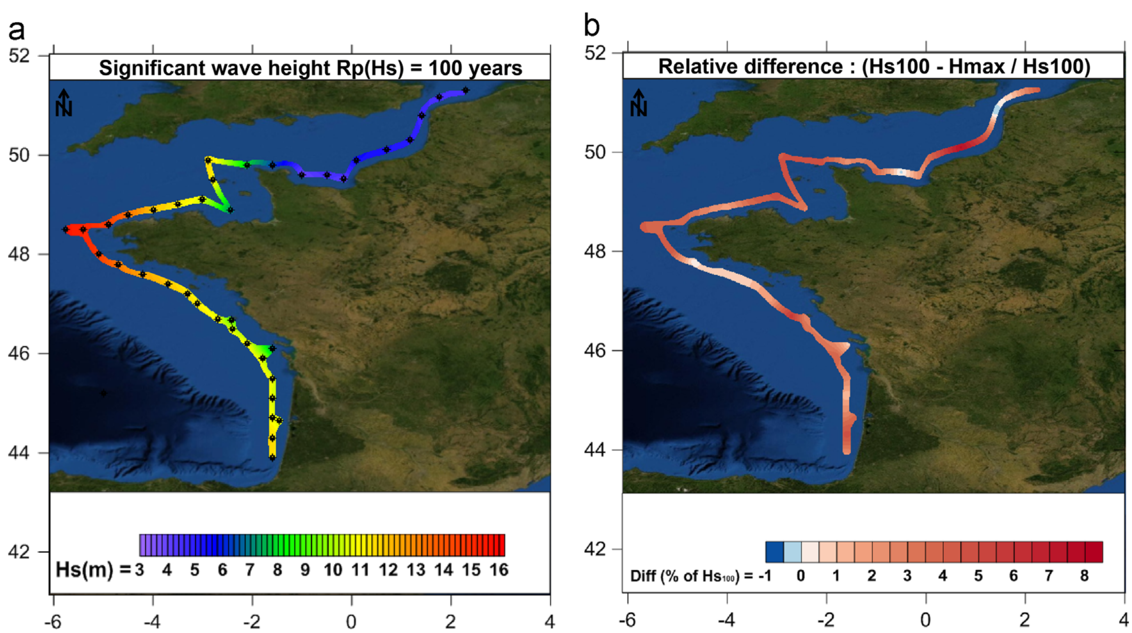

Fig. 6. Synthesis map at the national scale. (a) Variability of H_s values along the coast for a 100 year return period, (b) relative differences between H_{s100} and H_{smax} in the BoBWA-10 kH data base.

gradient along the northern and southern coasts that tends towards average values ($H_{s100} \approx 11$ m);

– The Loire–Vendée sector, with fairly medium average values (H_{s100} from 10 to 11 m);

– Aquitaine, also with average values that increase slightly along the Basque coast (H_{s100} from 10 to 12 m).

Along the Atlantic coast, the differences are mainly accounted for by the exposure of these French coastlines to large wave events and storms. As France mainland is particularly subjected to low pressure systems circulating from the west, waves higher than 7 m are frequent in the Bay of Biscay ($R_p < 1$ year). The values for $R_p = 1$ year even exceed 10 m at the westernmost point of Brittany. However, wave heights in the Channel are significantly lower. When waves come from the west, the entrance of the Channel is partly protected by the Cornish peninsula in England and the Breton peninsula in France. The height of waves coming into the Channel then gradually decreases as they reach shallower waters and land obstacles (Channel Islands, Cotentin peninsula). Large waves coming from low-pressure areas in the North Sea also flatten out as they cross the Dover Straits. Wave values for the eastern part of the Channel are therefore significantly lower than for the other French coastlines ($H_{s1} = 3$ to 3.5 m). The variations observed for other return periods (10, 30, 50 years, not shown), are very similar to the 100 year return period.

The difference between H_{s100} and the maximum value in the BoBWA-10 kH time series for each point is shown in Fig. 6b. A difference close to 0 suggests that historical events during the period simulated with BoBWA-10 kH have generated waves with a significant height close to the local 100-year value. These events are identified for each point in the BoBWA-X database and suggest that only South Brittany and the Dover Straits were concerned by H_s values close to H_{s100} during the covered period.

To further analyze the spatial variability of 100-year return period wave height, a depth-independent analysis of variations of the statistical parameters obtained for each point is performed. The shape parameter ξ drives the general behavior of the GPD and is dimensionless. It can be assumed to be independent of depth as in RFA where it represents the common extremal behavior of several sites inside a homogeneous region (Dalrymple, 1960). The scale parameter is expressed in meters and is dependent of depth. Therefore, it is adimensioned by the statistical threshold u_s which depends on the local characteristics of each site (u_s is related to a mean number of events per year $\lambda_s \simeq 2$): $\overline{\sigma} = \sigma / u_s$. This dimensionless scale parameter is similar to the regional scale parameter of Weiss et al. (2014a) used in a RFA framework. Fig. 7 shows the spatial variations of ξ and $\overline{\sigma}$ along the coast. Both parameters present a notable spatial variability. The analysis of ξ, resp. $\overline{\sigma}$, variations exhibits 7 quite homogeneous coastal segments where they are approximately constant (variations of ± 0.025 and ± 0.02 for ξ and $\overline{\sigma}$, respectively). Comparing both parameters, regions 4 to 7 have very similar delimitations, whereas regions 1 to 3 are slightly different. One hand, this can be explained by the different nature of the parameters: ξ characterize the overall climate, whereas $\overline{\sigma}$ characterize a more local behavior. In the English Channel, because of the wave propagation direction (mainly along the Channel) and a bi-directional regime, there should be many local effects, due to wave diffraction around headland for instance. One the other hand, in a RFA, both parameters would be constant by construction in each homogeneous segment. Here we still see some variations within segments. This can be partly explained by the slight fluctuations of the mean number of events per year λ_s (see Section 4) according to the sites which introduces heterogeneity in the analysis, but it also indicates the difficulty to define homogeneous regions where single regional scale and shape parameters would apply. However, the frontiers drawn in Fig. 7 are only indicative of the locations where significant changes of ξ or $\overline{\sigma}$ are noticed. Yet, the resulting segments can be interpreted physically. Indeed, if we compare this segmentation with the delimited areas on the H_{s100} spatial variations map (Fig. 6a), the same frontiers are identified, with a higher degree of precision for the segmentation based on the statistical parameters (7 segments versus 4 areas). This is because they are directly related to the wave climate and the exposure to classical storm waves of each homogeneous segment and they are not influenced by the bathymetry contrary to H_{s100}.

As a result, the Western Brittany area is divided into three segments thus separating the North (within the Channel and

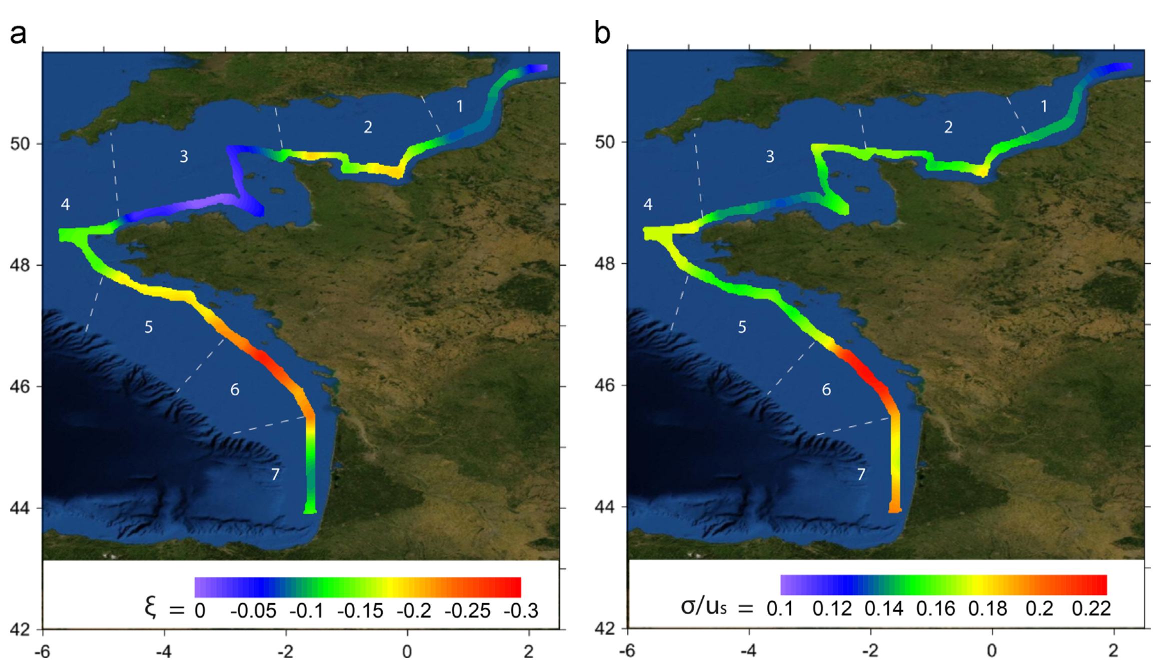

Fig. 7. Variability of statistical parameters at national scale. (a) parameter ξ (scale parameter), (b) parameter σ/u_s (shape parameter adimensioned by u_s). The delimitation of the 7 coastal segments is based on a visual analysis of the statistical parameters spatial variations.

partly protected from northwestern storms by the Cornish peninsula) from the West (open to the ocean) and from the South (not directly exposed to western and northwestern storm tracks). Similarly, the Channel east of the Cotentin peninsula is divided into two segments, one reason might be the stronger exposure of the northern segment to a bi-directional regime with waves coming from the Atlantic (West direction) and from the North Sea (North direction). Therefore, the method used to derive local extreme values of H_s provides physically relevant and regionally consistent statistical parameters.

5.2. Large wave events between 1958 to 2001: Extent and return periods

When crossing the BoBWA-10 kH database wave time series with the extreme wave heights (H_s) statistics database (BoBWA-X), 24 events with a theoretical return period $R_p(H_s)$ of more than 10 years were identified (Nicolae Lerma et al., 2014). Among them, seven events were identified where the wave heights has a theoretical return period higher than 50 years in at least one of the analyzed points. The spatial extent of these large wave events was reconstructed for the French Atlantic and Channel coasts (see Fig. 8). First, we can identify two groups: one with large waves located along the south part of the Atlantic coast (G1, containing events 1, 3, 5) and one with large wave located along the North Atlantic and English Channel coasts (G2, containing events 2, 4, 6, 7). The events identified do not correspond to a list of major storms which affected the French coasts, but correspond to the strongest wave events that have hit the French coastal area. These more or less localized events have alternately affected all the areas along the Atlantic and Channel coasts, indicating a clear regional distribution of large wave events. Brittany is the most exposed region in terms of number of events, with two events in the January 1958 – August 2002 period with 50-year wave heights or more. It seems, however, that $R_p(H_s) > 50$-yr events affecting the Bay of Biscay coasts have generated wave heights with a moderate return period ($R_p(H_s) < 10$-yr) in the Channel (e.g. 26/02/1989, Fig. 8) and vice versa (e.g. 15/12/1979). Among the events identified, there are no situation where observed waves with $R_p(H_s) > 10$-year occur simultaneously along the Channel coast (east of the Cotentin peninsula) and in the Bay of Biscay.

Two kinds of information emerge from the events identified: the extent of the coastline affected and the succession of major events. The extent of the coastline subject to large waves with $R_p(H_s) > 10$ years during the 15/12/1979 and 26/02/1989 events is quite remarkable. These events affected, respectively, more than 950 km of the Channel and Brittany coastline and 650 km of the Atlantic coast from Brittany to the Spanish border. However, they do not correspond to the episodes with the highest $R_p(H_s)$ values. The second important factor is the succession of major events within a few weeks or even a few days. In particular, during the year 1965 and in late 1989 and early 1990, a succession of very intense events was observed, triggered by particularly active low pressure systems circulating over northern Europe. During these events, all French coastlines were affected, with wave height return periods sometimes exceeding 100 years, for example during the Daria storm on 25/01/1990 in the Dover Straits area ($R_p(H_s) =$ 107 years).

The events identified show that the extent and intensity of large wave events can vary greatly from one event to another. Depending on local and regional characteristics (trajectory, size and intensity), a weather system can produce very different consequences in terms of wave conditions.

5.3. Relation with types of weather: Preliminary results

Relating spatial variability of waves to climate description is not straightforward when focusing on events occurring on a scale of few days. As a preliminary analysis, we investigate whether there are some characteristic meteorological patterns explaining the division of large wave events into the two groups G1 and G2 identified in Section 5.2. At seasonal scales, even if there is a significant positive correlation between wave heights of BoBWA-10 kH database and the NAO and EA phases for winter season

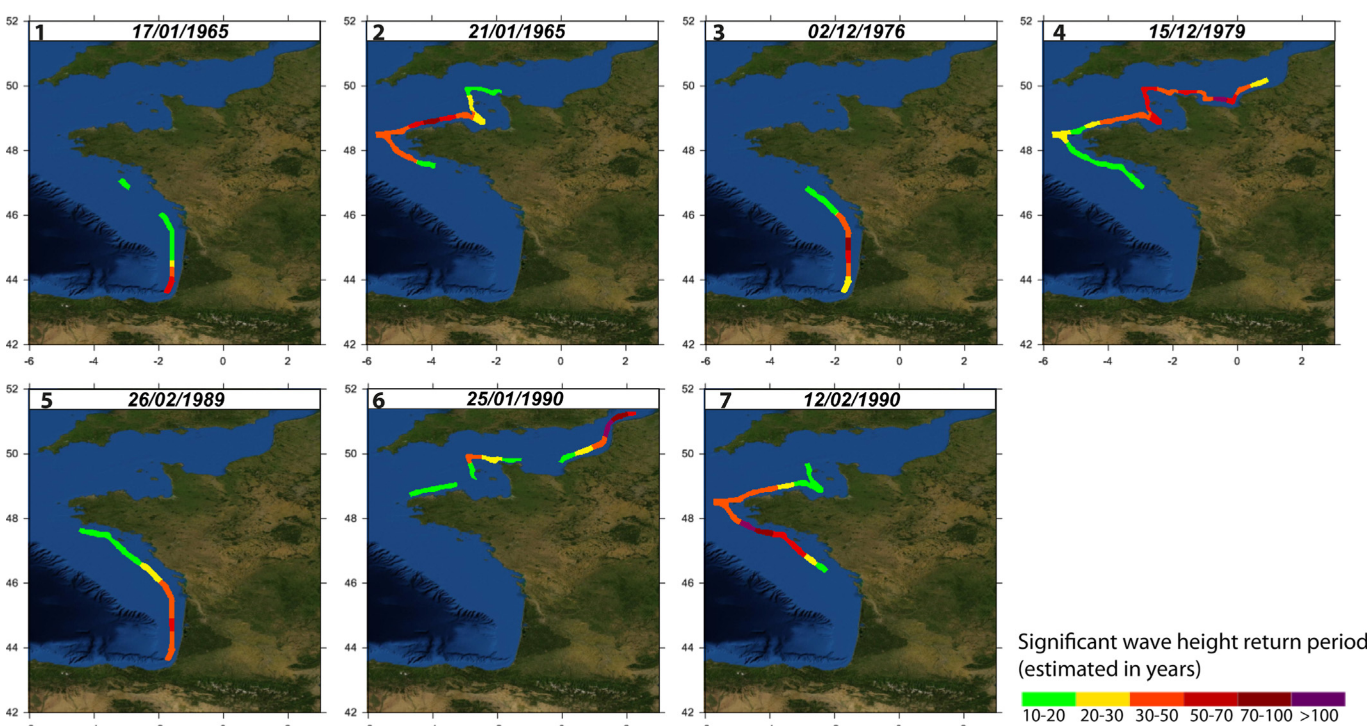

Fig. 8. Spatial extent of swell events detected in the BoBWA-10 kH data base, where $R_p(H_s) > 50$ years at least at one of the analyzed points.

(Charles et al., 2012), we don't observe specific relation for the winter associated to each event. Another approach to explain the division into G1 and G2 is to use weather type: Zonal (NAO+), Greenland Anticyclone (GA; NAO−), Blocking (BL) and Atlantic Ridge (AR). The analysis of the weather type occurring the day of the event (and the days before) does not exhibit any correlation between the weather type and the belonging of the swell event to group G1 or G2.

Last, we investigate whether there are some similarities between 3-day averaged mean-sea level pressure of each event (Fig. 9) leading to the same large wave group (G1 or G2). Indeed, several works have shown that a large proportion of the wave height anomalies in the northeast Atlantic are associated with pressure anomalies (e.g. Wang et al., 2010). First, considering group G1, the mean sea-level pressures of events 3 and 5 exhibit a pattern quite similar to AR pattern (low pressure at the North-East and high pressure at the South-East). For event 1, this is less clear. Focusing on group G2, two sub-groups are observed: one (events 2 and 4) with the lowest pressure located South-West of Island, the other one (events 6 and 7) with the lowest pressure located closer to Island and exhibiting a pattern similar to zonal (NAO+) pattern. Thus, as preliminary results, we observe a correlation between the 3-day averaged sea-level pressure and spatial variability of large wave events, nevertheless to link large wave spatial variability and climate variability, a proper statistical downscaling analysis based on a large enough number of weather types (e.g. 100) would be necessary (Laugel et al., 2014).

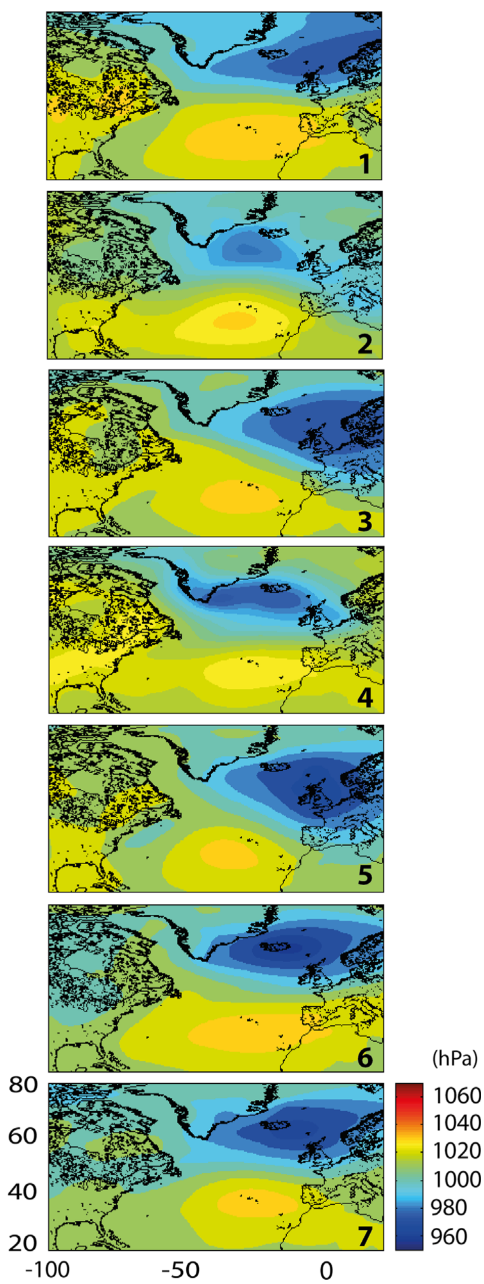

Fig. 9. Three-day averaged mean-sea level pressure of each events where $R_p(H_s) > 50$ years. Mean seal level pressure data source ERA-40 (Uppala et al., 2005).

6. Discussion

The return periods calculated in this study are theoretical values based on statistical laws and numerical wave data. Although the BoBWA-10 kH dataset has the characteristics required to calculate statistics for extreme conditions, analysis of the H_s peaks in the open sea simulated with BoBWA-10 kH shows a slight underestimation of about 4% compared to available data from buoys. It is important to remember that the majority of the analyzed points, and all of those shown in Fig. 1, are grid points forcing occur at 6-h intervals and wave data are exploited every 6 h. This resolution cannot produce a perfect representation of all wave peaks, hence a potential underestimation of H_s values. A comparison with 9 points with hourly output wave data showed that the relative difference between the two series (1-h and 6-h intervals) averages about 2% and is always within the 95% confidence interval for statistical adjustments. The maximum relative difference is observed for the Biscay_10 point (see Fig. 1 location 44.7°N; −1.6°E), at 4.2% of the 100-year value, or 0.48 m (Bulteau et al., 2013b).

In particular, the results obtained in the Channel should be considered with caution. Indeed, the influence of currents and tidal heights on wave characteristics is not taken into account in the model and the configuration used to build up the BoBWA-10 kH database. As the tidal range can vary from 2 to 12 m and currents from 0.25 to 5 m/s (SHOM, 2000), the reproduction of waves in the Channel is necessarily imperfect. Ardhuin et al. (2012) shown significant changes in wave characteristics in shallow water sectors with strong tidal currents, for example between the islands off the tip of Brittany or in the bays of St Malo and Mont St Michel. At present, HOMERE, covering the period 1994–2012 (Boudière et al., 2013), is the only wave database taking into account wave–current interactions for modeling waves in the Channel. This kind of model can be useful to improve reproducing wave conditions in strongly varying tidal and current area. With a longer covered period, it might help refining extreme wave heights statistics in the Channel. Nevertheless, results from the BoBWA-10 kH model for the Minquiers buoy are particularly good, suggesting that the waves are reasonably well represented.

Finally, it should be noted that the database covers a period of 44.7 years up to the year 2002. This duration is considered long enough to extrapolate probability distributions up to a return period of about 170 years while keeping statistical uncertainties manageable (4 times the period of observations, Pugh, 2004). However, this statistical analysis of extreme values does not cover more recent events, such as the Klaus storm of 24 January 2009. Wave heights during the Klaus storm (January 2009), particularly in the Gironde and Landes areas (southern Bay of Biscay), were extremely high with H_s recorded at Cap Ferret buoy 03302 (location 44.39°N; −1.27°E) of up to 11.7 m (CETMEF, 2012). This value is higher than the 100-year value determined by BoBWA-X for this point, but still within the 95% confidence interval. Therefore, should this value be included in the analysis, it would have a significant impact on local statistics raising the issue of updating databases on extremes in the case of exceptionally severe events of limited spatial extent. Nevertheless, more generally, recent events (2002–2013) have been of relatively moderate intensity, with wave heights below the 10-year return values determined by BoBWA-X for the Biscay and Minquiers buoys. It may therefore be considered that given the available observations, including the large wave events of the last 10 years, recent events would only have a marginal effect on the extreme values produced in BoBWA-X.

7. Conclusion

A new database of extreme wave values called BoBWA-X was created for French coasts using the BoBWA10-kH hindcast.

The validation showed that the BoBWA10-kH database is suitable for analyses of extreme values. Overall, compared to other existing regional databases for French coastlines, the characteristics of BoBWA10-kH data are closer to observations. The Quantile/Quantile analysis and the relationships established for storm peaks also demonstrated the capacities of the database for reproducing large wave events.

The statistical processing method implemented in the study is inspired by the approach of Bernardara et al. (2014) for POT samples. It requires the selection of a physical threshold value to decluster the data (i.e. make them independent) and then a higher statistical threshold on the basis of a series of tests that should enable to converge objectively towards an appropriate threshold. From the successive tests, the operator can confirm or reject the selection of pre-determined thresholds. By using only one distribution (i.e., the GPD) and one parameters' estimation method, this protocol is designed to allow comparisons between results obtained from the analysis of different points and to highlight the spatial variability of extreme wave characteristics on the scale of a region. The choice of the method of moments (MOM) to estimate GPD parameters was based on the characteristics of the data processed (sample size of around 100 records and negative shape parameter). In other circumstances, e.g. if ensuring a uniform approach to get spatially comparable results is not the purpose, it would be useful to test several estimation methods and to choose the method that produces the best fit.

The obtained extreme wave heights exhibit a significant spatial variability with 4 distinct areas, with 100-year return wave heights ranging between 3 m (East Cotentin) and 16 m (Western Brittany). A depth-independent analysis of the results observing the variations of the statistical shape parameter (ξ) and the dimensionless scale parameter ($\overline{\sigma}$), presents a notable spatial variability which delineates 7 quite homogeneous coastal segments where they are approximately constant (variations of ± 0.025 and ± 0.02 for ξ and $\overline{\sigma}$, respectively). The delimited segments are directly related to the wave climate and the exposure to classical storm waves. Therefore, they show similar repartition frontiers with the delimited areas by the H_{s100} spatial variations but with a higher degree of precision (7 segments versus 4 areas).

The study also produced an analysis of the intensity and extent of past large wave events, characterising the return periods of wave conditions associated with major events. The results describe events which have potentially affected the French coast during the second half of the 20th century. More extensive research will have to be considered to deepen our understanding of the relationships between spatial variability of large wave conditions at the coast and the trajectories of low pressure systems over northern Atlantic. It is worthwhile to remind that a strong large wave event is not necessarily synonymous of severe coastal erosion and flooding. Conversely, coastal flooding is not necessarily associated with large waves (e.g. Xynthia storm, Bertin et al., 2012). An in-depth analysis of the concomitance of tides, storm surges and waves would help developing plausible extreme scenarios at regional scale to better prevent erosion and coastal flood hazards.

Acknowledgements

The authors wish to thank Elodie Charles for the use of the BoBWA 10-kH waves database she developed for her thesis (financed by the AXA research fund), under a collaborative project between the BRGM and CNRM-GAME (Météo-France—CNRS). We also thank the DGPR (Ministry for Ecology, Sustainable Development and Energy) and BRGM (DAPP and DR) for co-funding the Wave Climate II study under which this project was undertaken. We thank François Paris for his comments and input during the Wave Climate l project. Finally, we thank the reviewer which comments improved this paper greatly.

References

Ardhuin, F., Chapron, B., Collard, F., 2009. Strong decay of steep swells observed across oceans. Geophys. Res. Lett. 36 (6), http://dx.doi.org/10.1029/2008GL037030 (art. no. L06607).

Ardhuin, F., Roland, A., Dumas, F., Bennis, A-C., Sentchev, A., Forget, P., Wolf, J., Girard, F., Osuna, P., Benoit, M., 2012. Numerical wave modeling in conditions with strong currents: dissipation, refraction, and relative windAm. Meteorolog. Soc. 42 (2101–2020)

Benoit, M., Lafon, F. Goasguen, G., 2006. Constitution et exploitation d'une base de données d'états de mer le long des côtes Françaises par simulation numérique sur 23 ans. In: Actes des IXèmes Journées Nationales Génie Côtier Génie Civil, Brest (France), September 12–14 , pp. 21–30. http://dx.doi.org/10.5150/jngcgc.2006.003-B.

Bernardara, P., Andreewsky, M., Benoit, M., 2011. Application of the Regional Frequency Analysis to the estimation of extreme storm surges. J. Geophys. Res. 116 (C02008), 1–11. http://dx.doi.org/10.1029/2010JC006229.

Bernardara, P., Mazas, F., Kergadallan, X., Hamm, L., 2014. A two-step framework for over-threshold modelling of environmental extremes. Nat. Hazard. Earth Syst. Sci. 14, 635–647. http://dx.doi.org/10.5194/nhess-14-635-2014.

Bertin, X., Dodet, G., 2010. Variabilité du climat de houle dans le Golfe de Gascogne au cours des six dernières décennies. In: Actes XIèmes Journées Nationales Génie Côtier Génie Civil, Sables d'Olonne (France), June 22–25, 2010. http://dx.doi.org/10.5150/jngcgc.2012.005-B.

Bertin, X., Bruneau, N., Breilh, J.-F., Fortunato, A.B., Karpytchev, M., 2012. Importance of wave age and resonance in storm surges: the case Xynthia, Bay of Biscay. Ocean Modell. 42, 16–30.

Boudière, E., Maisondieu, C., Ardhuin, F., Accensi, M., Pineau-Guillou, L., Lepesqueur, J., 2013. A suitable metocean hindcast database for the design of Marine energy converters. Int. J. Mar. Energy 3–4, e40–e52. http://dx.doi.org/10.1016/j.ijome.2013.11.010 (Publisher's official version).

Bulteau T., Lecacheux S., Nicolae Lerma A., Paris F., 2013a. Spatial extreme value analysis of significant wave heights along the French coast. In: Actes from International Short Conference on Extreme Value Analysis and Application to Natural Hazards (EVAN2013), Siegen, 8–11 September, pp. 46–56. ISSN 1868-6613.

Bulteau T., Nicolae Lerma A., Lecacheux S., 2013b. Projet Climats de houle—Phase 2: Analyse des valeurs extrêmes de vagues le long de la côte Atlantique et en Manche. Rapport final. BRGM/RP-62730-FR, 49p., 26fig., 3 ann. ⟨http://infoterre.brgm.fr/rapports/RP-62730-FR.pdf⟩.

Caires, S., Sterl, A., 2005. A new nonparametric method to correct model data: application to significant wave height from the ERA-40 re-analysis. J. Atmos. Oceanic Technol. **22**, 443–459. http://dx.doi.org/10.1175/JTECH1707.1.

CETMEF, 2012. Fiches synthétiques de mesure des états de mer, Centre d'Etudes Techniques Maritimes et Fluviales, Février 2012.

Charles, E., Idier, D., Thiébot, J., Le Cozannet, G., Pedreros, R., Ardhuin, F., Planton, S., 2012. Present wave climate in the Bay of Biscay: spatiotemporal variability and trends from 1958 to 2001. J. Clim. 25 (6), 2020–2039. http://dx.doi.org/10.1175/JCLI-D-11-00086.1.

Coles, S., 2001. An Introduction of Statistical Modelling of Extreme Values. Springer p. 228.

Dalrymple, T., 1960. Flood frequency method. U.S. Geological Survey Water Supply Papers 1543-A, 11–51.

Dee, D.P., et al., 2011. The ERA-Interim reanalysis: configuration and performance of the data assimilation system. Q. J. R. Meteorolog. Soc. 137, 553–597. http://dx.doi.org/10.1002/qj.828.

Duluc C-M., Deville Y., Bardet. L., 2014. L'évaluation des périodes de retour des niveaux marins extrêmes: application de la méthode des probabilités jointes aux ports de Brest et La Rochelle et analyse des incertitudes d'échantillonnage associées, La Houille Blanche, no. 1, pp. 11–17. http://dx.doi.org/10.1051/lhb/2014002.

Greenwood, P.E., Nikulin, M.S., 1996. A Guide to Chi-Squared Testing. Wiley, New York, NY.

Hawkes, P.J., Gonzales-Marco, D., Sánchez-Arcilla, A., Panayotis, P., 2008. Best practice for the estimation of extremes: a review. J. Hydraul. Res. 46 (2), 324–332.

Laugel, A., Menendez, M., Benoit, M., Mattarolo, G., Méndez, F., 2014. Wave climate projections along the French coastline: dynamical versus statistical downscaling methods. Ocean Modell. 84, 35–50. http://dx.doi.org/10.1016/j.ocemod.2014.09.002.

Lecacheux, S., Paris, F., 2013. Projet Climats de houle— phase 1: Intercomparaison de simulations rétrospectives et prospectives dans le Golfe de Gascogne, Rapport BRGM/RP-61651-FR, 116p., 58 ill, 1 ann. 〈http://infoterre.brgm.fr/rapports/RP-61651-FR.pdf〉.

Li, F., Bicknell, C., Lowry, R., Li, Y., 2012. A comparison of extreme wave analysis methods with 1994–2010 offshore Perth dataset. Coastal Eng. 69, 1–11. http://dx.doi.org/10.1016/j.coastaleng.2012.05.006.

Li, F., Van Gelder, P.H.A.J.M., Ranasinghe, R., Callaghanc, D.P., Jongejan, R.B., 2014. Probabilistic modelling of extreme storms along the Dutch coast. Coastal Eng. 86, 1–13.

Mackay, E.B.L., Challenor, P.G., Bahaj, A.S., 2011. A comparison of estimators for the generalised Pareto distribution. Ocean Eng. 38, 1338–1346.

Mathiesen, M., Hawkes, P., Martin, M.J., Thompson, E., Goda, Y., Mansard, E., Peltier, E., van Vledder, G., 1994. Recommended practice for extreme wave analysis. J. Hydraul. Res. 32, 803–814 (IAHR).

Martucci, G., Carniel, S., Chiggiato, J., Sclavo, M., Lionello, P., Galati, M.B., 2010. Statistical trend analysis and extreme distribution of significant wave height from 1958 to 1999—an application to the Italian Seas. Ocean Sci. 6, 525–538.

Mazas, F., Hamm, L., 2011. A multi-distribution approach to POT methods for determining extreme wave heights. Coastal Eng. 58, 385–394.

Méndez, F.J., Menéndez, M., Luceño, A., Losada, I.J., 2006. Estimation of the long-term variability of extreme significant wave height using a time-dependent peak over threshold (POT) model. J. Geophys. Res. 111, C07024.

Méndez, F.J., Tomas, A., Minguez, R., Reguero, B.G., 2011. A methodology to define extreme wave climate using reanalysis data bases. In: OEANS, 2011 IEEE – Santander Spain, 10pp. ISBN: 978-1-4577-0086-6.

Morton, I.D., Bowers, J., Mould, G., 1997. Estimating return period wave heights and wind speeds using a seasonal point process model. Coastal Eng. 31, 305–326.

Neelamani, S., Al-Salem, K., Rakha, K., 2007. Extreme waves for Kuwaiti territorial waters. Ocean Eng. 34 (10), 1496–1504 (July 2007).

Neelamani, S. (2009). Influence of threshold value on peak over threshold method on the predicted extreme significant wave heights in Kuwaiti territorial waters. In: Proceedings of the 10th International Coastal Symposium ICS 2009, 13–18 April 2009, Lisbon, Portugal, J. Coastal Res., Special Issue 56, Vol. 1, pp. 564–568.

Nicolae Lerma A., Bulteau T., Lecacheux S., Idier D., 2014. Période de retour des évènements de fortes houles le long des côtes françaises (Atlantique et Manche) entre 1958 et 2002. In: Actes des XIIIèmes Journées Nationales Génie Côtier Génie Civil, Dunkerque (France), 2–4 july, 10p.

Paris, F., Lecacheux, S., Idier, D., Charles, E., 2014. Assessing wave climate trends in the Bay of Biscay through an intercomparison of wave hindcasts and reanalyses. Ocean Dyn. 64, 1247–1267. http://dx.doi.org/10.1007/s10236-014-0746-1.

Pugh, C., 2004. Changing Sea Levels—Effects of Tides, Weather and Climate. Cambridge University Press, Cambridge.

Reguero, B.G., Méndez, F.J., Losada, I.J., 2013. Variability of multivariate wave climate in Latin America and the Caribbean. Global Planet. Change 100, 70–84.

SHOM, 2000, Tidal Streams and Tidal Heights: The Channel from Dunkerque to Brest, 564-UJA, ISN 2-11-088251-4.

Shorack G. R.,. Wellner J.A., 2009. Empirical Processes with Applications to Statistics, Philadelphie, Society for Industrial & Applied Mathematics, 4 September 2009, 998p.

Thompson, P., Cai, Y., Reeve, D., Stander, J., 2009. Automated threshold selection methods for extreme wave analysis. Coastal Eng. 56, 1013–1021.

Tolman, H.L., 2009. User Manual and System Documentation of WAVEWATCH III version 3.14, NOAA/NWS/NCEP/MMAB Tech. Note 276.

Uppala, S.M., et al., 2005. The ERA-40 re-analysis. Q. J. R. Meteorolog. Soc. 131, 2961–3012. http://dx.doi.org/10.1256/qj.04.176.

Wang, X.L., Swail, V.R., Cox, A., 2010. Dynamical versus statistical downscaling methods for ocean wave heights. Int. J. Climatol. 30, 317–332.

Weiss, J., Bernardara, P., Benoit, M., 2014a. Formation of homogeneous regions for regional frequency analysis of extreme significant wave heights. J. Geophys. Res. Oceans , http://dx.doi.org/10.1002/2013JC009668.

Weiss, J., Bernardara, P., Benoit, M., 2014b. Modeling intersite dependence for regional frequency analysis of extreme marine events. Water Resour. Res., 50. http://dx.doi.org/10.1002/2014WR01539.